Heliyon 10 (2024) e32540

Contents lists available at ScienceDirect

Heliyon

journal homepage: www.cell.com/heliyon

Research article

Determination of glucose oxidase activity by tyrosine fluorescence spectrophotometry

Aiju Zhang [b], Xiaolin Zhang [b], Lijing Yang [a], Fangzhen He [b,*], Xingde Dai [a,**], Na Dong [a,***]

[a] Department of Pharmacy, Gansu Medical College, Pingliang, Gansu, 744000, PR China
[b] Basic Chemistry Teaching Laboratory, Public Course Teaching Department, Gansu Medical College, Pingliang, Gansu, 744000, PR China

ARTICLE INFO

Keywords:
Glucose oxidase
Glucose
Hydrogen peroxide
Tyrosine
Fluorophotometry

ABSTRACT

A novel Fe^{2+}/Tyr/H_2O_2 fluorescence reaction system has been established for the purpose of analyzing glucose oxidase activity. This system involves the catalysis of glucose oxidase on glucose to produce H_2O_2, which in turn oxidizes tyrosine to a highly fluorescent substance under the catalysis of Fe^{2+}. The fluorescence intensity is subsequently employed to ascertain the enzymatic activity of glucose oxidase. The enzymatic oxidation reaction and tyrosine fluorescence reaction conditions were optimized based on the H_2O_2 standard curve equation. Direct fluorescence spectrophotometry was used to determine the activity range and detection limit of glucose oxidase, which were found to be 7.00×10^{-5}–7.00×10^{-2} U/mL and 3.36×10^{-5} U/mL (Enzyme-like activity is 6.72×10^{-4} U/mL, The enzyme reaction time is 5 min), respectively, with a relative standard deviation of less than 3.2 %. This method has been successfully applied to determine the activity of glucose oxidase in food additives, with a recovery rate ranging from 96.00 % to 102.0 %.

1. Introduction

Glucose oxidase (GOx) is an aerobic dehydrogenase found in molds such as Aspergillus niger, which can specifically oxidize β-D-glucose into gluconic acid and H_2O_2, consuming a large amount of oxygen to form an anaerobic environment [1–3]. It is widely used in food industries such as food deoxygenation in milk powder, wine, and juice, flour improvement, prevention of food browning, and rapid food testing [4–7], as well as in the preparation of medical products such as urine glucose test strips and blood glucose test strips [8–10]. In recent years, GOx has also been widely used in emerging fields such as biosensors [11,12], biofuels [13,14], and textile bleaching [15,16]. GOx is widely distributed in animals, plants, and microorganisms, and due to the fast reproduction and wide availability of microorganisms, they have become the main source of GOx [17–19].

As the application fields of GOx continue to expand, the demand in domestic and international markets has increased sharply. Therefore, the research on detection methods and material preparation related to GOx has important practical significance. In recent years, research related to this topic has certain reference value. For example, Zhang et al. [20]. developed a GOx-mediated sensing

* Corresponding author.
** Corresponding author.
*** Corresponding author.
E-mail addresses: hefangzhen2016@163.com (F. He), plyz_dxd@163.com (X. Dai), dongna886@163.com (N. Dong).

https://doi.org/10.1016/j.heliyon.2024.e32540
Received 28 March 2024; Received in revised form 15 May 2024; Accepted 5 June 2024
Available online 8 June 2024

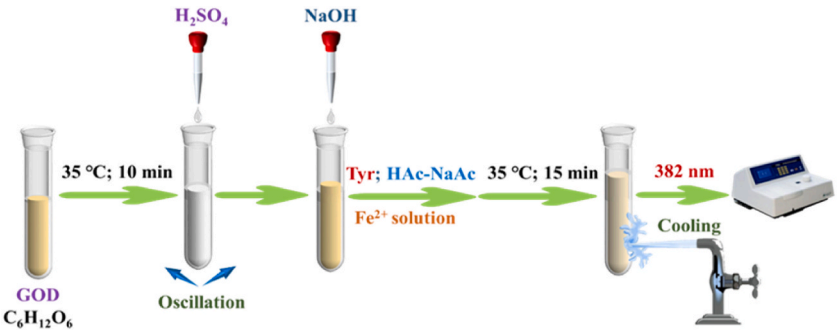

Fig. 1. Experimental process diagram.

system with a detection limit of 0.21 nM for glucose. This method is simple in design and low in cost. Another example is the colorimetric sensitive analysis technique for GOx by Griyte R et al. [21], which utilizes the photo-oxidation of TMB (3, 3′, 5, 5′-tetramethylbenzidine) catalyzed by semiconductor cadmium sulfide nanoparticles (NPs). The results showed that the sensitivity of colorimetric analysis is comparable to that of fluorescence analysis. Furthermore, Chaichi M J et al. [22]. immobilized GOx onto Fe_3O_4-chitosan nanoparticles to construct a novel and efficient glucose biosensor based on chemiluminescence detection of enzymatically produced H_2O_2. This provides technical support for the practical application of GOx.

However, the complexity, high cost, and low efficiency of the GOx detection process have become one of the factors limiting the industrial application of GOx [23–25]. Traditional detection methods include titration [26], electrode method [27], fluorescence photometry [28], etc. Although these methods have their own advantages, further research is needed to develop simpler and more efficient GOx detection methods. Among the many methods for detecting GOx activity, the use of fluorescence detection has rarely been reported. We have created a fluorescence reaction system based on the chemical reaction between the phenolic hydroxyl group in the molecular structure of tyrosine (Tyr) and the formation of fluorescent tyrosine dimers [29,30]. By relying on the Fe^{2+}/Tyr/H_2O_2 fluorescence reaction system, we have established a standard curve for H_2O_2, and then converted it into GOx activity through the working curve equation. This method for detecting GOx activity is simple, rapid, accurate, and has great practical value.

2. Experimental section

2.1. Instruments and reagents

In all experiments, a fluorescence photometer (360 nm excitation light source, Shanghai Tianmei Company) was utilized. The experimental solutions primarily consisted of glucose solution (100 mmol/L), Tyr solution (0.01 mmol/L, biochemical reagent, Aladdin), H_2O_2 standard solution (2.8 mmol/L), glucose oxidase working solution (50 μg/mL, Beijing Wokai Biotechnology Co., LTD.), $FeSO_4$ solution (1.0 mmol/L), and HAc-NaAc buffer solution (0.1 mol/L, pH = 5.00).

2.2. Drawing of H_2O_2 standard curve

Take six 10 mL cuvettes and add 0.00, 0.10, 0.20, 0.30, 0.40, 0.50 mL of 2.8 mmol/L H_2O_2 standard solution in sequence. Then add 1.00 mL of 0.01 mol/L Tyr solution, 2.00 mL of 0.1 mol/L HAc-NaAc (pH = 5.0) buffer solution, and 0.8 mL of 1.0 mmol/L $FeSO_4$ solution to each cuvette, diluted to the scale. React at 35 °C for 15 min, and cool to room temperature with running water. When the excitation wavelength is 360 nm, measure the fluorescence intensity F at the emission wavelength of 382 nm. Furthermore, plot the standard curve of H_2O_2 with concentration (C (μmol/mL)) as the abscissa and fluorescence intensity (ΔF) as the ordinate, and determine the slope k of the equation.

2.3. Determination of the enzyme activity

The definition of GOx activity entails the quantity of 1 U necessary to catalyze the glucose reaction, resulting in the production of 1 μmol of hydrogen peroxide (H_2O_2) within a duration of 1 min. The enzyme activity is denoted by unit U/mL. Design the following scheme based on the definition of enzyme activity, and derive the formula for calculating enzyme activity.

A 10 mL colorimetric tube was used to separately contain 1.00 mL of glucose oxidase sample solution (<0.025 U/mL) and glucose solution (0.1 mol/L). The mixture was then allowed to react at 35 °C for 5 min, after which 1.00 mL of pH = 2.00 sulfuric acid was added to terminate the enzyme-catalyzed reaction. The solution was thoroughly oscillated and pH = 12.00 sodium hydroxide (1.00 mL) was added to restore the solution environment to its original state, thus preparing the enzyme-catalyzed reaction solution. To this solution, Tyr solution (1.00 mL, 0.01 mol/L), HAc-NaAc buffer solution (2.00 mL, 0.1 mol/L, pH = 5.0) and Fe^{2+} solution (0.80 mL, 1.0 mmol/L) were added and the resulting mixture was diluted to the scale. After allowing the reaction to proceed at a temperature of 35 °C for a duration of 15 min. When exciting at a wavelength of 360 nm, measure the fluorescence intensity F at 382 nm. The experimental process is shown in Fig. 1.

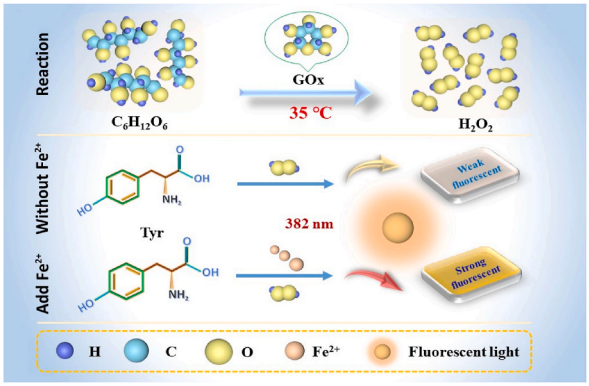

Fig. 2. Scheme of catalytic fluoresce detection of GOx activity.

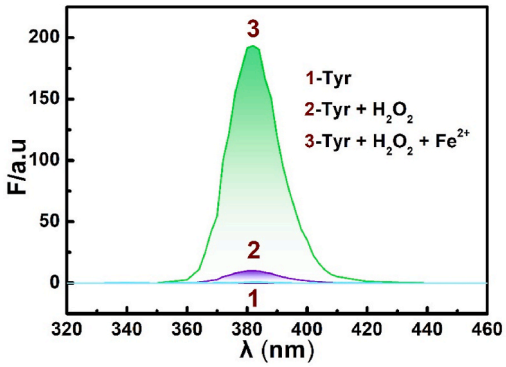

Fig. 3. Fluorescence curve when C (Tyr) = 1.0 mmol/L, C(H_2O_2) = 0.14 mmol/L, C(Fe^{2+}) = 0.08 mmol/L.

This measurement was taken after cooling the sample to room temperature using water. Additionally, the enzyme blank fluorescence intensity F_0 was determined. Using formula (1):

$$X = \frac{\Delta F}{k} \times 10 \times \frac{1}{t \times Vs} \tag{1}$$

The GOx activity X of the enzyme solution was calculated. The variables X, k, t, Vs, and 10 respectively represent the activity of the enzyme solution in U/mL, the slope of the H_2O_2 working curve in mL/μmol, the dilution of the enzyme solution by a factor of 10, the enzymatic catalytic reaction time in minutes, and the sample liquid volume of GOx in mL. The difference between F and F_0 is represented by ΔF.

3. Results and discussion

3.1. Reaction principle

Under the catalysis of GOx, glucose is oxidized to produce H_2O_2. In pH5.0 acetate buffer solution, using Fe^{2+} as a catalyst, the generated H_2O_2 reacts with Tyr to form Tyr dimers. The specific reaction process is as follows:

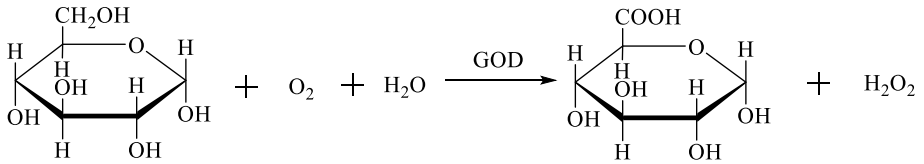

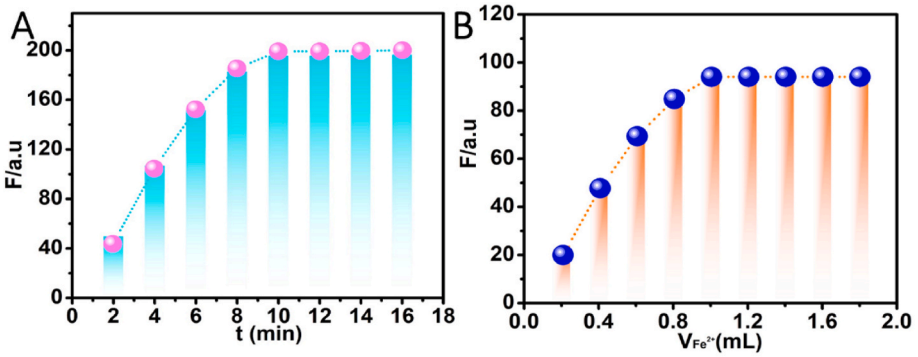

Fig. 4. Effect of A) heating time and B) amount of Fe^{2+} on the fluorescence reaction when C(H_2O_2) = 0.14 mmol/L, C (Tyr) = 1.0 mmol/L.

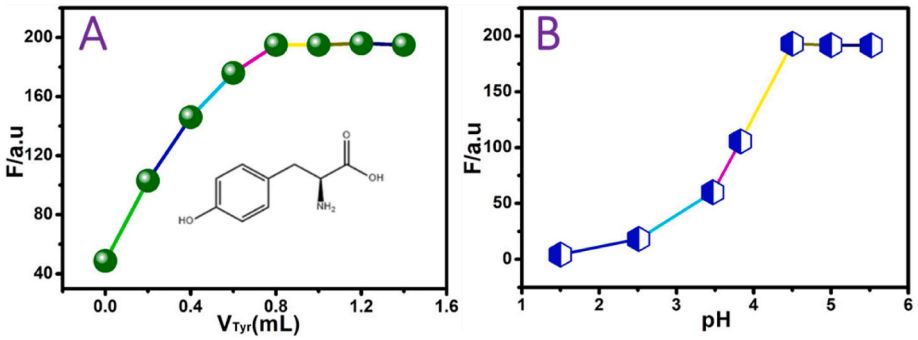

Fig. 5. Effect of A) Tyr dosage and B) pH on the fluorescence reaction when C(H_2O_2) = 0.14 mmol/L, t = 10 min, C(Fe^{2+}) = 0.08 mmol/L.

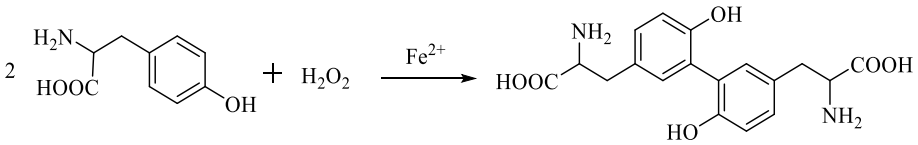

The strong fluorescent effect of Tyr dimer occurs at a wavelength of 382 nm. It is well known that the fluorescent intensity of Tyr dimer is directly proportional to the concentration of H_2O_2 within a certain range. Based on this, we performed two reactions: GOx catalyzed oxidation of glucose and enzyme solution with Tyr. We then measured the fluorescent intensity at a wavelength of 382 nm, and calculated the change in fluorescent intensity (ΔF) before and after adding the enzyme solution. By substituting this value into the H_2O_2 working curve equation, we were able to estimate the activity of GOx. The principle of this measurement is illustrated in Fig. 2.

3.2. The emission curve of the tyrosine dimer products

The emission curve depicting the tyrosine dimer products is illustrated in Fig. 3. It is observed that Tyr exhibits weak fluorescence, as shown in Curve 1. Additionally, the reaction between Tyr and H_2O_2 is also weak, resulting in a small fluorescence peak at a wavelength of 382 nm (Curve 2). Upon catalysis by Fe^{2+}, Tyr undergoes oxidation by H_2O_2, leading to the formation of Tyr dimer, which exhibits a strong fluorescence signal release. Notably, the emission wavelength remains at 382 nm, as depicted in Curve 3. The indirect fluorescence of Tyr is attributed to the strong oxidation of fenton reagent ($Fe^{2+} + H_2O_2 \rightarrow Fe^{3+} + HO\bullet + OH^-$) and the unique structure of Tyr, The oxidation products of Tyr exhibit long conjugated $\pi \rightarrow \pi^*$ transitions, resulting in an increase in fluorescence intensity [31]. Furthermore, the fluorescence intensity is closely related to H_2O_2, which is generated through the catalytic oxidation of glucose by GOx. This provides a reliable basis for the determination of GOx activity.

3.3. Optimization of tyrosine fluorescence reaction conditions

A standard solution of H_2O_2, measuring 0.50 mL and with a concentration of 2.8 mmol/L, was utilized in lieu of the enzyme catalyzed reaction solution. The fluorescence reaction of Tyr was examined through a single factor method, with a focus on the impact of reaction time, reaction temperature, Fe^{2+} concentration, dosage of Tyr, and solution acidity. The aforementioned reaction exhibits

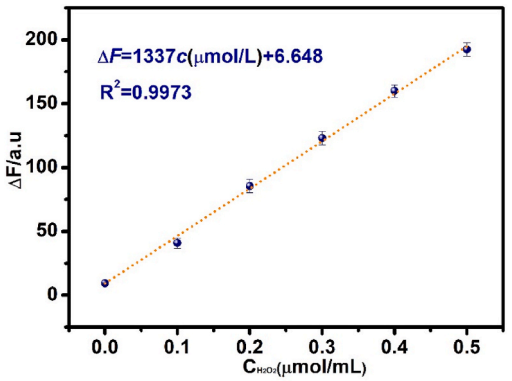

Fig. 6. Relationship between H_2O_2 concentration and solution fluorescence intensity when C(H_2O_2) = 0.14 mmol/L, C (Tyr) = 1.0 mmol/L, t = 10 min, C(Fe^{2+}) = 0.08 mmol/L, pH = 5.0.

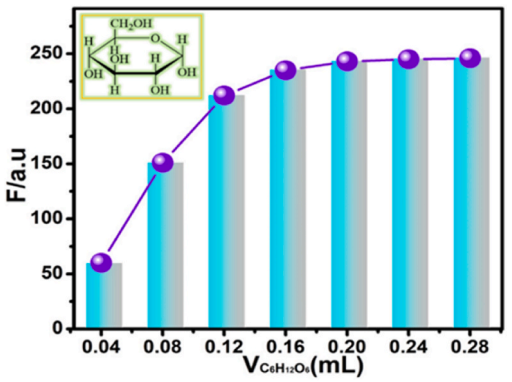

Fig. 7. The relationship between glucose dosage and fluorescence intensity under optimized H_2O_2 and Tyr fluorescence reaction conditions.

conformity with the enzyme-catalyzed oxidation reaction, and the application of water bath heating proved to be conducive to expediting the fluorescence reaction. Following a reaction period of 10 min at a temperature of 35 °C, the generation of Tyr dimer reached its maximum, and the fluorescence intensity remained constant. As a result, the heating duration is determined to be 10 min (Fig. 4A). The Fenton reagent is formed through the combination of Fe^{2+} and the enzyme-catalyzed oxidation product H_2O_2. Even a small quantity of Fe^{2+} (0.08 mmol/L) exhibits a potent catalytic ability. To mitigate the side reactions caused by Fe^{2+}, a volume of 0.80 mL of Fe^{2+} is employed for a concentration of 1.0 mmol/L (Fig. 4B).

The concentration of Tyr was varied across a range of values (0, 0.05, 0.1, 0.2, 0.3, 0.4, 0.5, 0.8, 1.0 mmol/L) and its impact on the mixed solution's *F* value was studied (Fig. 5A). The findings indicate that *F* increased as the concentration of Tyr increased within the range of 0.05–0.8 mmol/L. However, when the concentration of Tyr exceeded 0.8 mmol/L, the mixture's *F* value remained largely unchanged. To ensure a relative excess of Tyr, the optimal concentration of 1.0 mmol/L was selected for this experiment. Therefore, 1.00 mL of Tyr was extracted from 0.01 mol/L for testing purposes.

The findings presented in Fig. 5B demonstrate the impact of solution pH on the oxidation reaction of Tyr. The amine group (-NH_2) in the structure of Tyr dimer was found to be protonated, leading to a weakened fluorescence signal. As a result, high acidity was found to be unfavorable for the formation of Tyr dimer. Optimal fluorescence was observed at a solution pH of 4.5–5.5. However, excessive alkalinity resulted in the conversion of Fe^{2+} into $Fe(OH)_3$ precipitation. Therefore, the experiment utilized a HAc-NaAc buffer solution with a pH of 5.0 as the reaction medium, with the addition of 1.00 mL.

3.4. Analysis of H_2O_2 standard curve

Determine the optimal conditions for fluorescence reaction, and plot the H_2O_2 working curve according to the method described in "2.3", as shown in Fig. 6. The results indicate that there is a linear relationship between the concentration of H_2O_2 and the change in fluorescence intensity (ΔF) within the range of 1.40×10^{-4}–0.14 μmol/mL, with a corresponding relationship equation of $\Delta F = 1337c$ (μmol/mL) + 6.648 and a correlation coefficient of 0.9973. Continuously measure the H_2O_2 blank solution 11 times, and the measured values are 0.8, 0.8, 0.8, 0.8, 0.8, 0.8, 0.7, 0.8, 0.8, 0.8, 0.8. Calculate the standard deviation S = 0.03, and then use 3 times the deviation value divided by the slope of the working curve to obtain the detection limit of H_2O_2 (D = 6.73×10^{-5} μmol/mL).

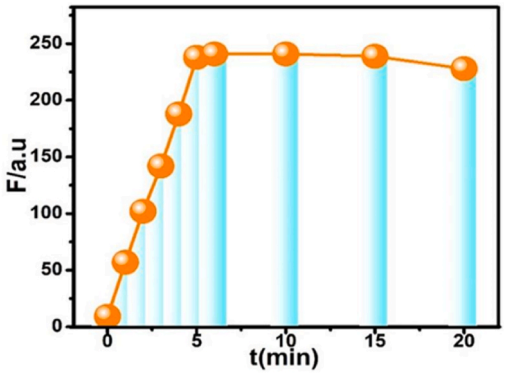

Fig. 8. The relationship between enzyme catalytic reaction time and fluorescence intensity under optimized H_2O_2 and Tyr fluorescence reaction conditions.

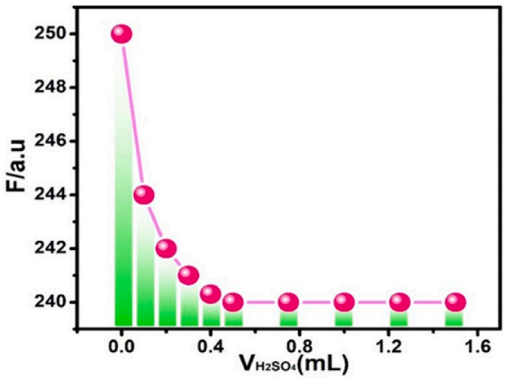

Fig. 9. Under the optimized conditions of the H_2O_2 and Tyr fluorescence reaction, the relationship between the amount of H_2SO_4 and fluorescence intensity.

3.5. Optimization of the enzyme-catalyzed oxidation reaction conditions

(1) Determination of the glucose volume of the bottom fluid

From a reaction principle standpoint, it can be observed that the reaction ratio between the substrate glucose and the probe Tyr is 1:2. However, it is important to note that the enzyme-catalyzed reaction is a zero-order reaction, and only a fraction of the enzyme reaction, specifically 1/5, participates in the fluorescence reaction. As a result, it can be inferred that glucose must be present in excess, at a minimum of 2.5 times that of Tyr.

A volume of 0.10 mL of GOx working liquid (50 μg/mL) and 0.1 mol/L glucose solution were utilized as substrates, with their volumes being varied from 0.00 to 1.00 mL. Following a 10-min enzyme-catalyzed reaction, the fluorescence reaction was completed using method "2.3″ and the fluorescence intensity was measured (Fig. 7). The findings indicate that *F* increases proportionally with the volume of glucose solution, with *F* reaching its maximum when the volume of glucose solution exceeds 0.20 mL. The glucose oxidase-catalyzed reaction is a quasi-first-order reaction, with the reaction rate being independent of the substrate concentration. A substrate of 0.1 mol/L glucose solution with a volume of 1.00 mL was employed for the enzyme-catalyzed reaction.

(2) Optimization of the enzyme catalytic reaction time

By utilizing 0.10 mL of a 50 μg/mL working solution of glucose oxidase, modify solely the reaction time and execute the fluorescence reaction in accordance with the prescribed methodology outlined in "2.3". Subsequently, ascertain the fluorescence intensity. The enzyme-catalyzed reaction rate curve was then generated, utilizing time t as the abscissa and *F* as the ordinate, as depicted in Fig. 8.

The enzyme-catalyzed reaction proceeded rapidly within a time frame of 5 min, as evidenced by the linear relationship between *F* and t, which reflects the characteristics of an enzyme-catalyzed first-order reaction. Subsequently, after the initial 5-min period, the growth rate of *F* decelerated in tandem with the decrease of dissolved oxygen volume. It is noteworthy that the activity of glucose oxidase enzyme is indicative of the rate of H_2O_2 production rather than the amount of H_2O_2 production. As such, the enzyme-catalyzed

Table 1
Precision experiment.

Samples	1	2	3	4	5	6
ΔF	160.5	161.7	163.9	162.8	167.6	166.5
Activity (U/mL)	0.2407	0.2426	0.2459	0.2443	0.2515	0.2498
Mean activity (U/mL)	0.2458					
RSD/%	1.70					

Table 2
Selective experiment for enzyme activity determination.

Experimental Serial Number	Add enzyme (50 μg/mL)	Add enzyme volume (mL)	Activity Assay (U/mL)	Measurement error/%
1	–	–	0.2458	–
2	Amylase	0.10	0.2517	2.40
3	Catalase	0.10	0.2050	−16.60
4	Horseradish peroxidase	0.10	0.2496	1.55
5	Alkaline phosphatase	0.10	0.2536	3.17
6	Sucrose invertase	0.10	0.2534	3.10

reaction time has been set at 5 min.

(3) Enzyme catalytic reaction termination test

The rate of H_2O_2 production, rather than its amount, is reflected by the activity of GOx enzyme. Therefore, it is crucial to terminate the enzyme-catalyzed reaction in a timely manner. Although both boiling the enzyme solution and strengthening the acid and alkali can achieve this purpose, they have an impact on the subsequent fluorescence reaction. The former results in the decomposition of H_2O_2, while the latter is not conducive to the formation and fluorescence release of Tyr dimer. The novel approach employs a combination of strong acid and alkali, wherein 1.00 mL of sulfuric acid solution with a pH of 2.00 is introduced during the initial stage to promptly halt the enzyme-catalyzed oxidation reaction. Following thorough oscillation, the sulfuric acid is neutralized by the addition of an equal volume of pH 12.00 sodium hydroxide. The experimental results validate that the addition of sulfuric acid solution with a pH of 2.00 exceeding 0.50 mL can instantaneously inactivate the enzyme solution, and the method employs precisely 1.00 mL of the solution (Fig. 9).

(4) Linear range and detection limit of GOx

The range of linearity and limit of detection for H_2O_2 are 1.40×10^{-4} to 0.14 μmol/mL and 6.73×10^{-5} μmol/mL, respectively. The rate of enzyme-catalyzed reaction is reflected by the activity of GOx. Therefore, by setting the catalytic oxidation reaction time of GOx to 5 min, the determination range and detection limit of GOx activity can be established at 7.00×10^{-5} to 7.00×10^{-2} U/mL and 3.36×10^{-5} U/mL, respectively.

3.6. Precision experiments

The working liquid containing 50 μg/mL of GOx was subjected to activity measurement for 6 consecutive times, and the corresponding results were presented in Table 1. The enzyme exhibited an average activity of 0.2458 U/mL, and an actual activity of 4913 U/g. The relative standard deviation (RSD) was calculated to be 1.70 %, indicating that the fluorescence spectrophotometry method employed in the determination of GOx activity was highly accurate.

3.7. Selective experiment

Take 0.10 mL of the 50 μg/mL working solution of glucose oxidase, and add amylase, catalase, horseradish peroxidase, alkaline phosphatase, and invertase of the same mass concentration to investigate interference. The results indicated that except for catalase, other enzymes had no impact on the determination of the activity of glucose oxidase, and the relative error (RE) of the measurement was less than 5 % (Table 2). The GOx in food additives is originated from Aspergillus niger, and catalase is generally not generated during its preparation process, thus it can be disregarded.

3.8. Sample analysis

Accurately weighed samples of 0.05 g retail enzyme solid (food grade, labeled amount 2000 U/g, Yuwanbang) were placed in a 100 mL volumetric bottle and dissolved with a pH of 7.0 phosphoric acid buffer solution for constant volume. The solution was then magnetically stirred for 30 min. After centrifuging at 6000 r/min for 5 min, the supernatant was collected and diluted 50 times, 100

Table 3
Sample analysis and recovery experimental results.

Samples	Configuration concentration (mg/mL)	Activity measurement (U/mL)	RSD (%)	Spiked (U/mL)	Measured Value (U/mL)	Recovery (%)
1	0.0100	0.0450	3.2	0.0100	0.0546	96.00
2	0.0050	0.0224	2.6	0.0200	0.0428	102.0
3	0.0025	0.0155	1.6	0.0300	0.0447	97.33

times, and 200 times with phosphoric acid buffer solution to obtain 0.0100 mg/mL, 0.0050 mg/mL, and 0.0025 mg/mL sample solutions. The samples were determined according to the "2.3″ method, and a standard recovery experiment was conducted. The results of the experiment are presented in Table 3.

The observed recoveries exhibit a range of 96 %–102 %, with a relative standard deviation (RSD) of less than 3.2 %. These results suggest that the method employed in this study is characterized by high levels of accuracy and precision.

4. Conclusion

This paper presents a novel approach to detecting GOx activity using tyrosine fluorescence reaction. The method significantly enhances sensitivity, accuracy, and operability, with an enzyme activity detection range of 7.00×10^{-5} to 7.00×10^{-2} U/mL and a detection limit of 3.36×10^{-5} U/mL. This makes it more suitable for trace analysis of biological samples compared to photometric methods, with a better width. The proposed method lays a theoretical foundation for the development of GOx fluorescence kits. In the subsequent improvement process, two aspects should be prioritized for breakthroughs. Firstly, enzymatic reaction time can be further optimized by adjusting the amount of glucose substrate. Secondly, a more ideal catalyst than Fe^{2+} should be identified to improve the stability of the detection system.

CRediT authorship contribution statement

Aiju Zhang: Funding acquisition, Data curation. **Xiaolin Zhang:** Project administration, Formal analysis. **Lijing Yang:** Funding acquisition. **Fangzhen He:** Writing – review & editing, Software, Resources. **Xingde Dai:** Writing – original draft. **Na Dong:** Investigation, Data curation, Conceptualization.

Declaration of competing interest

The authors declare no competing financial interest.

Acknowledge

This work was performed with the financial support of Gansu Medical College (GY-2023FZZ06).

References

[1] A. Prévoteau, N. Mano, How the reduction of O_2 on enzymes and/or redox mediators affects the calibration curve of "wired" glucose oxidase and glucose dehydrogenase biosensors, Electrochim. Acta 112 (2013) 318–326.
[2] J.A. Bauer, M. Zámocká, J. Majtán, et al., Glucose oxidase, an enzyme "Ferrari": its structure, function, production and properties in the light of various industrial and biotechnological applications, Biomolecules 12 (3) (2022) 472–497.
[3] J.F. Kornecki, D. Carballares, P.W. Tardioli, et al., Enzyme production of D-gluconic acid and glucose oxidase: successful tales of cascade reactions, Catal. Sci. Technol. 10 (17) (2020) 5740–5771.
[4] A. Abdi, A. Karimi, M. Razzaghi, Continuously deoxygenation of water in a reactor packed with glucose oxidase immobilized in MnO_2/calcium alginate composite, J. Environ. Chem. Eng. 4 (2) (2016) 2356–2361.
[5] A. Kothapalli, K. Hayes, G. Sadler, et al., Comparison of kinetic profile of free and immobilized glucose oxidase, immobilized on low-density polyethylene using UV polymerization, J. Food Sci. 72 (9) (2007) C478–C482.
[6] T. Yang, Y. Bai, F. Wu, et al., Combined effects of glucose oxidase, papain and xylanase on browning inhibition and characteristics of fresh whole wheat dough, J. Cereal. Sci. 60 (1) (2014) 249–254.
[7] S.H. Khatami, O. Vakili, N. Ahmadi, et al., Glucose oxidase: applications, sources, and recombinant production, Biotechnol. Appl. Biochem. 69 (3) (2022) 939–950.
[8] M. Bekhit, H.Y. Wang, S. McHardy, et al., Infection screening in biofluids with glucose test strips, Anal. Chem. 92 (5) (2020) 3860–3866.
[9] J. Lankelma, Z. Nie, E. Carrilho, et al., Based analytical device for electrochemical flow-injection analysis of glucose in urine, Anal. Chem. 84 (9) (2012) 4147–4152.
[10] P. Mandpe, B. Prabhakar, H. Gupta, et al., Glucose oxidase-based biosensor for glucose detection from biological fluids, Sens. Rev. 40 (4) (2020) 497–511.
[11] N. German, A. Ramanaviciene, A. Ramanavicius, Dispersed conducting polymer nanocomposites with glucose oxidase and gold nanoparticles for the design of enzymatic glucose biosensors, Polymers 13 (13) (2021) 2173.
[12] C. Chen, H. Xu, Q. Zhan, et al., Preparation of novel HKUST-1-glucose oxidase composites and their application in biosensing, Microchim. Acta 190 (1) (2023) 10.
[13] T. Bahar, Development of reasonably stable chitosan based proton exchange membranes for a glucose oxidase based enzymatic biofuel cell, Electroanalysis 32 (3) (2020) 536–545.
[14] L. Zhang, O.M. Manley, D. Ma, et al., Enhanced P450 fatty acid decarboxylase catalysis by glucose oxidase coupling and co-assembly for biofuel generation, Bioresour. Technol. 311 (2020) 123538.

[15] K. Mojsov, Enzymatic desizing, bioscouring and enzymatic bleaching of cotton fabric with glucose oxidase, J. Textil. Inst. 110 (7) (2019) 1032–1041.
[16] A. Madhu, J.N. Chakraborty, Bio-bleaching of cotton with H2O2 generated from native and immobilized glucose oxidase, AATCC J. Res. 6 (2) (2019) 7–17.
[17] Y.H. Hu, C.Z. Wang, Glucose oxidase in insects and its function, Chin. Bull. Entomol. 46 (3) (2009) 337–343.
[18] D. Tian, M. Peiffer, E. Shoemaker, et al., Salivary glucose oxidase from caterpillars mediates the induction of rapid and delayed-induced defenses in the tomato plant, PLoS One 7 (4) (2012) e36168.
[19] C.J. Carter, R.W. Thornburg, Tobacco nectarin V is a flavin-containing berberine bridge enzyme-like protein with glucose oxidase activity, Plant Physiol. 134 (1) (2004) 460–469.
[20] J. Zhang, C. Yang, C. Chen, et al., Determination of nitrite and glucose in water and human urine with light-up chromogenic response based on the expeditious oxidation of 3, 3′, 5, 5′-tetramethylbenzidine by peroxynitrous acid, Analyst 138 (8) (2013) 2398–2404.
[21] R. Grinyte, G. Garai-Ibabe, L. Saa, et al., Application of photocatalytic cadmium sulfide nanoparticles to detection of enzymatic activities of glucose oxidase and glutathione reductase using oxidation of 3, 3′, 5, 5′- tetramethylbenzidine, Anal. Chim. Acta 881 (2015) 131–138.
[22] M.J. Chaichi, M. Ehsani, A novel glucose sensor based on immobilization of glucose oxidase on the chitosan-coated Fe_3O_4 nanoparticles and the luminol-H_2O_2-gold nanoparticle chemiluminescence detection system, Sens. Actuators, B 223 (2016) 713–722.
[23] P. Wu, Q. Shao, Y. Hu, et al., Direct electrochemistry of glucose oxidase assembled on graphene and application to glucose detection, Electrochim. Acta 55 (28) (2010) 8606–8614.
[24] S. Jiang, Y. Zhang, Y. Yang, et al., Glucose oxidase-instructed fluorescence amplification strategy for intracellular glucose detection, ACS Appl. Mater. Interfaces 11 (11) (2019) 10554–10558.
[25] T. Li, D. Deng, D. Tan, et al., Immobilized glucose oxidase on hierarchically porous COFs and integrated nanozymes: a cascade reaction strategy for ratiometric fluorescence sensors, Anal. Bioanal. Chem. 414 (20) (2022) 6247–6257.
[26] Q. Lang, L. Yin, J. Shi, et al., Co-immobilization of glucoamylase and glucose oxidase for electrochemical sequential enzyme electrode for starch biosensor and biofuel cell, Biosens. Bioelectron. 51 (2014) 158–163.
[27] W. Wang, X. Zhang, J. Wang, The influence of local glucose oxidase activity on the potential/current distribution on stainless steel: a study by the wire beam electrode method, Electrochim. Acta 54 (23) (2009) 5598–5604.
[28] S.K. Shukla, A.K. Mishra, B.B. Mamba, et al., Amperometric and photometric responses of in situ coupled glucose oxidase-poly (propylene imine) dendrimer based glucose biosensor, Int. J. Electrochem. Sci. 8 (10) (2013) 11711–11722.
[29] M. Tyminski, K. Ciacka, P. Staszek, et al., Toxicity of meta-Tyrosine, Plants 10 (12) (2021) 2800.
[30] Z. Xu, X. Qiao, R. Tao, et al., A wearable sensor based on multifunctional conductive hydrogel for simultaneous accurate pH and tyrosine monitoring in sweat, Biosens. Bioelectron. 234 (2023) 115360.
[31] Y. Zhao, J. Long, P. Zhuang, et al., Transforming polyethylene and polypropylene into nontraditional fluorescent polymers by thermal oxidation, J. Mater. Chem. C 10 (3) (2022) 1010–1016.